How to cite: *Angew. Chem. Int. Ed.* **2021**, *60*, 21457–21463
International Edition: doi.org/10.1002/anie.202107277
German Edition: doi.org/10.1002/ange.202107277

Bioinorganic Chemistry

Biomimetic Iron Complex Achieves TET Enzyme Reactivity**

*David Schmidl[+], Niko S. W. Jonasson[+], Eva Korytiaková[+], Thomas Carell, and Lena J. Daumann**

Abstract: *The epigenetic marker 5-methyl-2′-deoxycytidine (5mdC) is the most prevalent modification to DNA. It is removed inter alia via an active demethylation pathway: oxidation by Ten-Eleven Translocation 5-methyl cytosine dioxygenase (TET) and subsequent removal via base excision repair or direct demodification. Recently, we have shown that the synthetic iron(IV)-oxo complex $[Fe^{IV}(O)(Py_5Me_2H)]^{2+}$ (**1**) can serve as a biomimetic model for TET by oxidizing the nucleobase 5-methyl cytosine (5mC) to its natural metabolites. In this work, we demonstrate that nucleosides and even short oligonucleotide strands can also serve as substrates, using a range of HPLC and MS techniques. We found that the 5-position of 5mC is oxidized preferably by **1**, with side reactions occurring only at the strand ends of the used oligonucleotides. A detailed study of the reactivity of **1** towards nucleosides confirms our results; that oxidation of the anomeric center (1′) is the most common side reaction.*

Introduction

5-methyl-2′-deoxycytidine (5mdC), an epigenetic marker, is the most common natural DNA modification.[1] The corresponding nucleobase, 5mC, is also referred to as the fifth base, in addition to the canonical bases A, T, C and G. 5mdC is generated in the mammalian genome primarily but not solely in CpG dinucleotides via methylation of cytosine by DNA methyl transferases.[1,2] Most of these CpG dinucleotides (up to 80%) are methylated, although they remain largely unmodified when located in CpG islands within promotor regions.[3] 5mdC levels are fairly stable making up to 5% of all cytosines in adult mammalian cells.[4] However, their fate is much more dynamic in embryonic stem cells during the early stages of development.[5,6] 5mdC levels are regulated either via dilution during cell division (referred to as passive demethylation) or via a stepwise oxidation mechanism where 5mdC is converted to 5-hydroxymethyl-2′-deoxy-cytidine (5hmdC), 5-formyl-2′-deoxy-cytidine (5fdC), and 5-carboxy-2′-deoxy-cytidine (5cadC) by Ten-eleven Translocation 5-methyl cytosine Dioxygenases (TET, active demethylation).[7–10] 5fdC and 5cadC are then removed either via base excision repair or via direct demodification.[9,11] TET belongs to the superfamily of non-heme iron(II)/α-ketoglutarate (α-KG) dependent enzymes. These enzymes possess a conserved active site that consists of the so-called facial triad (two histidine residues and one carboxylate-containing amino acid, in the case of TET: glutamate) that coordinates to an iron ion. The coordination sphere is completed by coordination of the co-factor α-KG, water, or oxygen.[12,13] During activation, α-KG is converted to succinate while an iron(IV)-oxo species (see Figure 1 left) is generated.[14–16] This iron(IV)-oxo moiety is believed to be the active species that abstracts a hydrogen atom from the substrate, generating an iron(III)-hydroxo species and a carbon-centered radical. These then recombine to form the hydroxylated product.[17] Multiple iron(IV)-oxo complexes have been used as model systems to mimic natural processes.[18–24] The iron(IV)-oxo complex utilized in this work ($[Fe^{IV}(O)(Py_5Me_2H)]^{2+}$ (**1**), Py_5Me_2H = 2,6-bis(1,1-bis(2-pyridyl)ethyl)pyridine, counterions: F^-, OH^-, NO_3^-) was first described by Chang et al. in 2015.[25] **1** is soluble in water, air-stable, and does not decompose within several hours at room temperature.[25] We have recently demonstrated that **1** is capable of mimicking the behavior of TET enzymes by oxidizing the nucleobase 5mC to 5hmC, 5fC and 5caC. By comparing the reaction rates of **1** with those published for TET2,[26] we were able to conclude that the second coordination sphere of TET enzymes is one important factor responsible for its substrate preference. Furthermore, GC/

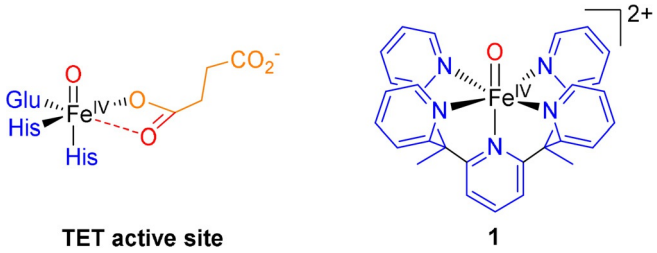

TET active site 1

Figure 1. The active site of TET enzymes (left), highlighted in blue is the facial triad, in red are the two oxygen atoms that originate from molecular dioxygen and in orange is the remainder of the α-KG co-substrate.[12] Right: Biomimetic iron(IV)-oxo complex **1** used in this study with the active oxo moiety shown in red.

[*] D. Schmidl,[+] N. S. W. Jonasson,[+] E. Korytiaková,[+] T. Carell, L. J. Daumann
Department Chemie, Ludwig-Maximilians-University München
Butenandtstr. 5–13, Haus D, München (Germany)
E-mail: lena.daumann@lmu.de
[+] These authors contributed equally to this work.
[**] Ten-eleven translocation 5-methylcytosine dioxygenase.
Supporting information and the ORCID identification number(s) for the author(s) of this article can be found under: https://doi.org/10.1002/anie.202107277.

MS and UV-vis studies confirmed hydrogen atom abstraction to be the rate determining step.[27]

The selective oxidation or reduction of cytosine derivatives in DNA is a highly desired transformation for in vitro processes, such as the sequencing of epigenetic bases. Whilst several chemical methods have been published for the oxidized bases,[28–32] the controlled conversion of 5mC still poses a challenge due to the low reactivity of the methyl group and its chemical similarity to the sugar scaffold. Selective oxidation is even more desirable as the current gold standard for single-base 5mC sequencing, the bisulfite method,[33] is destructive to the DNA sample[34,35] and is not able to intrinsically distinguish 5mC/5hmC and C/5fC/5caC.[28,36–39] Hence, the reactivity of TET enzymes presents a useful tool demonstrated by TAB-Seq[40] (TET-assisted bisulfite sequencing) for 5hmC and TAPS[41] (TET-assisted pyridine-borane sequencing) for 5mC and 5hmC. Nevertheless, the handling of TET enzymes is non-trivial and one major drawback of these methods is the large amount of enzyme required (sometimes more than stoichiometric amounts[40]). Moreover, the substrate specificity in terms of sequence bias/sequence preference and divergent reactivity against ssDNA and dsDNA might limit the utility of enzyme-based approaches. This technological example illustrates that a chemical strategy mimicking the reactivity of TET enzymes might benefit in vitro, and potentially even in vivo, applications for selective oxidation of 5mdC. In the present work we show that the substrate scope of **1** includes nucleosides and oligonucleotides. We show that **1** is capable of selectively oxidizing a 5mdC residue within a 10-mer oligonucleotide context. We also present a comprehensive study of the reactivity of **1** towards nucleosides including side reactions affecting the ribose unit.

Results and Discussion

After the successful demonstration of the oxidation of the nucleobase 5mC by **1**, we wanted to take a step towards nucleosides and actual DNA oligonucleotides as a substrate to evaluate the potential of **1** for biomimetic-TET-based sequencing methods. We therefore studied the reactivity of **1** towards a short oligomer (10-mer) containing a 5mdC residue (see Figure 2).

Oligonucleotide Substrates

We chose an oligonucleotide sequence which is composed of deoxyadenosines, deoxycytidines, deoxyuridines and deoxyguanosines, as these nucleobases do not contain aliphatic hydrocarbons that are prone to be attacked by **1**. Deoxyuridines were included instead of thymidines, as the methyl group of thymine is, of course, a possible target for oxidation by **1**. As 5mdC residues occur in nature, mostly in CpG dinucleotides, we included this into our oligonucleotide design and therefore chose the following sequence (5′- > 3′): HO-CCUUAACC**5mdC**G-OH (**O**). When **O** was exposed to **1** (1.0 or 4.0 equiv) we detected significant amounts of the

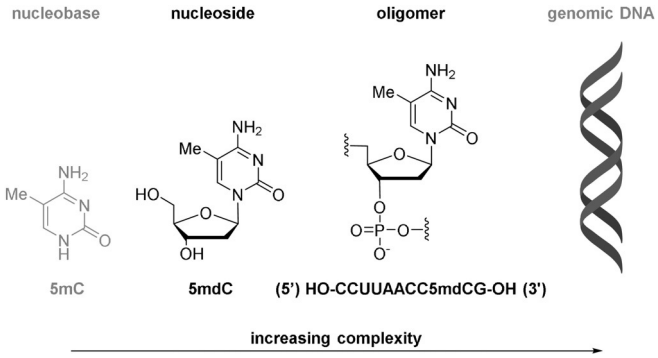

Figure 2. The increasing complexity of the substrate: from nucleobase via nucleoside and oligonucleotide to genomic DNA. In this work we present results from reactions containing nucleosides and oligonucleotides.

oxidized derivatives of 5mdC (For experimental details please see supporting information sections 1.6, 1.8 and 3). Figure 3 shows the amounts detected for 5mdC, 5hmdC, 5fdC and 5cadC in two samples containing both **O** and **1** (1 equiv **1**, 4 equiv **1**) as well as two control samples (**O** control, **1** control) that only contain the specified component. The common oxidative DNA lesion 8-oxo-dG was not observed (not shown, see Figure S27).

As observed in Figure 3, higher amounts of iron complex **1** generally result in higher levels of 5hmdC, 5fdC and 5cadC. This is pronounced least for 5hmdC and most for 5cadC, which points to a sequential oxidation process. It should be noted, that levels for 5hmdC and 5fdC are 10-fold higher than

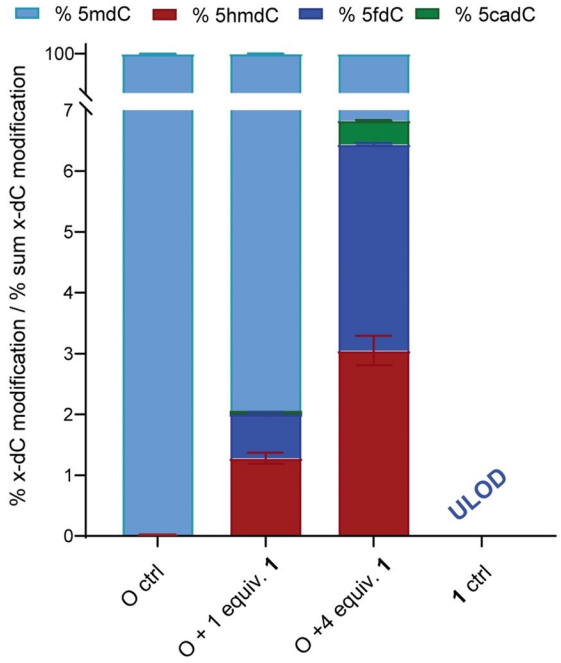

Figure 3. Detected amounts of 5hmdC, 5fdC, 5cadC when **O** was reacted with 1.0 equiv of **1** (O + 1 equiv **1**) or 4.0 equiv of **1** (O + 4 equiv **1**) compared to control measurements containing only **O** (**O** ctrl) or **1** (**1** ctrl) that were treated exactly as the samples. Conditions: [**O**] = 0.25 mM, [**1**] = 0.25 mM/1.0 mM, H_2O, T = 22 °C, reaction time = 30 min. ULOD refers to under level of detection.

for 5cadC. This circumstance indicates both a stepwise oxidation process and a higher reactivity of 5hmdC vs. 5fdC (see also section on nucleoside substrates).

8-oxo-dG is a common oxidative DNA lesion that can cause base mismatching.[42,43] The formation of 8-oxo-dG is a potential side-reaction in oxidative treatment of DNA, as dG presents the lowest oxidation potential of the canonical bases.[44] However, this was not observed in the case of **O**: 8-oxo-dG levels are under the level of detection (ULOD) for all samples including control samples (Figure S27). Thus, we conclude that 8-oxo-dG is not formed upon treatment of oligonucleotides with **1**.

Additionally, we tracked the time-resolved development of 5mdC, 5hmdC, 5fdC, and 5cadC levels in the reaction of **1** with **O**. 5mdC levels decrease (Figure S28) whereas levels of 5hmdC and 5fdC increase sharply immediately after addition of **1** (Figure 4). 5cadC levels also increase but to a much smaller extent. It is noteworthy that the final concentrations observed in these experiments match the concentrations observed in the experiments described above (Figure 3): 5hmdC and 5fdC are about 10-fold more abundant than 5cadC. This shows that the method is reproducible. The circumstance where we detected different ratios for 5hmdC/5cadC and 5fdC/5cadC (see Figure S29) when using different amounts of **1**, hints that the amount of **1** added can be used to stir the product formation of the reaction. Additionally, the development of the product ratios over time indicates that the reaction time may provide a similar method of influencing the product distribution for possible sequencing applications (Figure S29). The concentration of the substrate (0.125–0.25 mM) in the experiments discussed above was set at these levels so that the results are comparable with our previous studies and the reactions with nucleosides as substrates described below. For a biochemical application, the substrate concentrations need to be adjusted accordingly.[27]

Further studies with 5mdC residues within larger oligomeric structures, double-stranded substrates, and at lower substrate concentrations are necessary, but our findings give a first insight into the usefulness of **1** in the controlled oxidation of methylated or oxomethylated DNA samples, for example, for sequencing applications. In contrast to the previously studied nucleobases, oligonucleotides present more than one point of possible attack: the methyl group on the nucleobase itself or the carbohydrate (deoxyribose) backbone can be subject to C–H activation. We therefore screened for possible side products (see Section 3.6 in the SI). Reaction mixtures were analyzed prior to enzymatic digestions for any of the target nucleosides (dG, 8-oxo-dG, dU, dC, 5mdC, 5hmdC, 5fdC, 5cadC) using triple QQQ mass spectrometry, however, detected levels were found to be below the limit of detection.

MALDI MS measurements show that the strand ends are oxidized upon exposure of **O** to **1**, but no internal strand-breaks occur (Figures S30–S39). We did detect the loss of ≈95 *m/z* and ≈135 *m/z* which would correspond to loss of a cytosine or guanine nucleobase fragment while simultaneously an oxygen atom is gained (Figures S32 and S34, Scheme S4). A likely mechanism is the oxidation of the 1′ position of the terminal nucleotides (deoxycytidine on the 5′ end, deoxyguanosine on the 3′ end) with subsequent loss of the nucleobase and formation of a lactone (Scheme 1 A). We also observed loss of ≈291 *m/z* (Figures S31, S33), which was

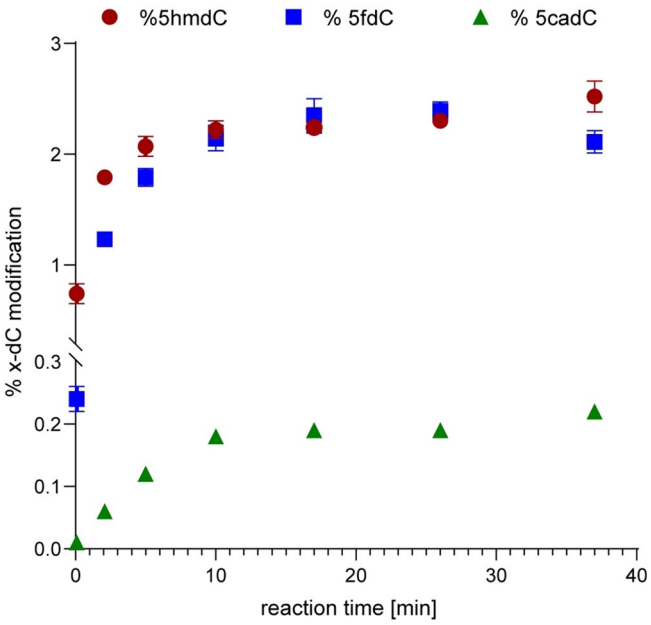

Figure 4. Time-resolved monitoring of the reaction of **O** with **1**: detected amounts of 5hmdC, 5fdC, 5cadC after certain time intervals. Conditions: [**O**] = 0.125 mM, [**1**] = 0.5 mM, H_2O, T = 22 °C. Data points are averaged from two replicates, each sample was measured in three technical replicates. For a separated representation of these data, including 5mdC levels, see Figure S28.

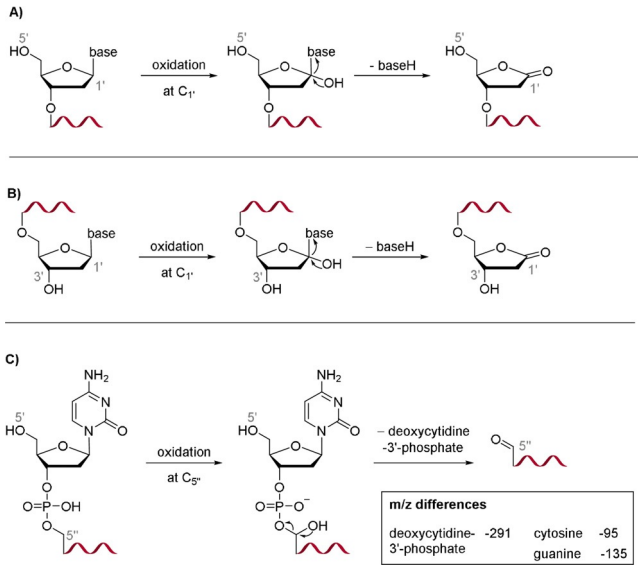

Scheme 1. A) Proposed mechanism for the loss of a nucleobase via oxidation of the 1′ position of the terminal deoxyribose unit on the 5′ end. B) Proposed mechanism for the loss of a nucleobase via oxidation of the 1′ position of the terminal deoxyribose unit on the 3′ end. C) Proposed mechanism for the loss of deoxycytidine-3′-phosphate via oxidation of the 5′-site of the second-to-last deoxyribose unit on the 5′ end of the strand (see Figures S30–S39 and Scheme S4 for a more detailed side product analysis).

assigned to the oxidation of the 5′ position of the second-to last ribose unit on the 5′ end of the strand resulting in the loss of a cytidine-3′-phosphate fragment (Scheme 1B). We performed the same experiments with a control strand that contains a dC residue instead of 5mdC, and the same control strand that in addition possesses a phosphate cap on the 5′ end (for sequence details see Table S4). We observed significantly more side reactions in both cases (see Figures S36–S39). This confirms that oxidation at the 5-position of cytosine in the case of **O** is preferred over the side-reactions.

Interestingly, in all samples we observed either the loss of two cytosine fragments or the loss of one guanine and one cytosine fragment but never any interior strand breaks. This supports our interpretation that only the terminal positions on the oligonucleotide are subject to side reactions, demonstrating the highly specific reactivity of **1**.

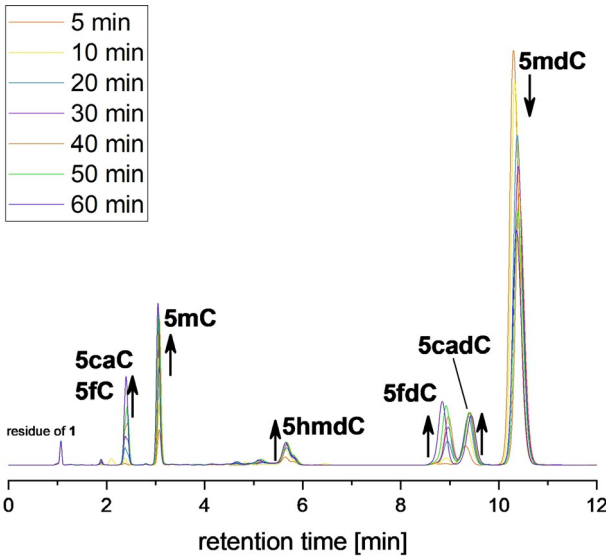

Figure 5. Excerpt of a representative HPLC trace of the reaction of 5mdC with **1**. Conditions: [5mdC] = 1 mM, [**1**] = 5 mM, H_2O, T = 22 °C. For a more detailed assignment see Figures S2–S10.

Nucleoside Substrates

To obtain a clearer picture of the competing reactivity of the potential oxidation sites in oligonucleotides, including confirmation of the above proposed side reaction pathways, we analyzed the reactivity of **1** towards the nucleoside substrates 5mdC and 5hmdC. Overall, we found that while the 1′ position on the deoxyribose unit is indeed oxidized forming the 2′-deoxyribono-γ-lactone, the 5-position on the cytosine base is oxidized faster yielding mostly the 5-oxomethylated cytidine derivatives 5hmdC, 5fdC, and 5cadC. We first conducted a series of reactions between 5mdC and different equivalents of **1**, for either 15 min or 30 min, to estimate how much and where the nucleoside with its high number of potential reactive sites would be oxidized. A color change from green to orange was observed during these reactions, indicating consumption of the green iron(IV)-oxo species **1**. Independent from the reaction time and the amount of added oxidant, we observed the 5-oxidized 5mdC derivatives 5hmdC, 5fdC, and 5cadC as the main products (Figure 5, Figure S17).

The relative abundance of nucleoside products reflects a correlation between the oxidation kinetics of the cytosine 5-substituent with the respective C–H bond dissociation energies (BDEs, see Table S5), as determined in previous studies with **1** and the nucleobases: 5hmC reacts the fastest, followed by 5mC and lastly 5fC.[27] Interestingly, these results are in opposition to those reported for TET enzymes (TET2), for which the following reaction rate sequence was found: $k_{5mC} > k_{5hmC} > k_{5fC}$.[26] While the behavior of TET2 was attributed to an additional interaction of the DNA substrate with a secondary coordination sphere in the enzyme,[27] the observed nucleoside product distribution in the reaction with **1** is in line with the consensus oxidation mechanism proposing an initial hydrogen atom transfer from the substrate to the iron(IV)-oxo species as the rate-determining step.[17,27] The corresponding nucleobases were detected on lower levels while practically no further side products, e.g., through oxidation at various deoxyribose carbons, were present in the product mixtures. Due to their similar BDEs, the anomeric center at the 1′ position of the nucleosides (BDE: 87.7 kcal mol^{-1})[45] might react with a similar rate as the most rapidly oxidized hydroxymethyl group of 5hmC (BDE: 86.2 kcal mol^{-1}).[26] This would lead to oxidative hydrolysis of the nucleoside (Scheme 2A, also compare Scheme 1A and B), constituting one possible explanation for the detection of nucleobase products upon addition of **1** to 5mdC. To confirm $C_{1'}$-oxidation, we subjected one such reaction mixture to GC/MS analysis and found 2′-deoxyribono-γ-lactone, the expected $C_{1'}$-oxidation side product, next to all four nucleobases (see inset in Scheme 2). It should be noted that the bases can not only be formed by oxidation of the anomeric center, but also

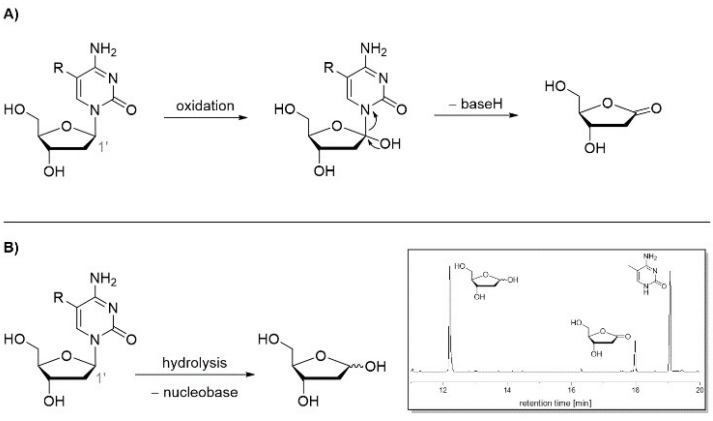

Scheme 2. A) Proposed mechanism for the loss of a modified cytosine nucleobase fragment from a nucleoside substrate via oxidation of the 1′ position of deoxyribose unit resulting in the formation of 2′-deoxyribono-γ-lactone. B) Proposed, although unlikely, hydrolysis of a modified cytidine nucleoside. A representative GC-MS trace is shown, the signals that were assigned to deoxyribose, 2′-deoxyribono-γ-lactone, and 5mC are indicated (see Figures S18–S22 for a more detailed analysis).

via "normal" hydrolysis of the *N*-glycosidic bond, which might occur both during the reaction or the work-up process. Indeed, we also detected high amounts of 2′-deoxyribose; however, this is not a suitable indication for hydrolysis happening during the reaction as the nucleosides hydrolyze during the derivatization process prior to GC analysis. Since this has generally only been reported to happen under very acidic conditions[46] or with the use of enzymes,[47] it appears unlikely to have occurred in this case. By filtering a mixture of the four nucleoside standards through silica followed by freeze-drying and HPLC analysis, we could rule out that the work-up contributed significantly to nucleoside hydrolysis. Further, the side product analysis for the oligonucleotide reaction (Scheme 1 C) suggests that $C_{5'}$-oxidation also occurs which appears feasible due to the similar BDE to the 5-formyl group (BDEs: 92.4 kcal mol^{-1},[45] 92.9 kcal mol^{-1},[26] respectively). Such products might correspond to the remaining peaks observed in the HPLC chromatogram, however, those are so small that we propose the corresponding oxidation reactions to happen only to a very low extent, leaving anomeric center oxidation as the most prominent proposed side reaction on a nucleoside substrate.

To obtain a more detailed image of the progress of the oxidation reaction, 5mdC was reacted with 5 equivalents of **1** and the reaction tracked over 70 min by taking samples every 5 min (Figure 6, Scheme S1). Whereas the amount of recovered 5mdC decreased throughout the course of the reaction, the 5hmdC concentration reached a steady state at as low as < 5 % of recovered products after 25 min, indicating that it is more rapidly oxidized than 5mdC. Accordingly, the amount of 5fdC formed increased fast to reach its steady-state concentration between 7–9 % of recovered products, equally after 20–25 min, which shows that it is less quickly consumed than 5hmdC. In line with the proposed stepwise oxidation mechanism, significant 5cadC levels (i.e., three oxidation steps taking place) are detectable after 10 min at the earliest. Also, it seems that 5cadC is accumulated over the entire 70 min without reaching a steady state concentration within this timeframe. Nevertheless, 5mC levels reach up to 16 % and 5caC levels even add up to 18 % of recovered products, indicating that anomeric center oxidation is a significant side reaction on the nucleoside level.

Interestingly, the reaction of 5mdC with **1** seems to proceed much slower than that of **1** with the oligonucleotide **O**: The nucleoside reaction proceeds throughout the monitored 70 min time frame (Figure 6) while the reaction between **O** and **1** appears to be complete after 10–12.5 min (Figure 4)—even though the concentration of 5mdC is 8-fold higher than that of **O** and 5 equivalents of **1** are used for the nucleoside compared to 4 equivalents on the oligonucleotide. An explanation for this could be electrostatic attraction between negatively charged **O** and the iron(IV)-oxo cation bringing the reaction partners into spatial proximity. Additionally, π-stacking interactions might be feasible between the nucleobases and the aromatic pyridyl-based ligand of **1**.

An analogous time-resolved experiment of the reaction between 5hmdC with **1** was conducted (Figures S23, S24, Scheme S2). According to BDEs and previous experiments,[26,27] the hydroxymethyl group should react considerably faster than the methyl group of 5mdC, eventually leading to much higher levels of 5cadC. Additionally, more information might be gained about the relative reactivity of the anomeric center with its BDE being very similar to the hydroxymethyl group. Indeed, 5hmdC was much more rapidly converted than 5mdC, with only 46 % recovered already after 5 min, while it became almost completely consumed over the full 70 min (about 2.5 % recovery). In parallel, 5fdC was very swiftly formed, reaching its maximum concentration after about 10 min (ca. 45 % recovery) after which its concentration decreased again due to the formation reaction slowing down (ca. 20 % recovery after 70 min). 5cadC, which was already detected after 5 min, accumulated rapidly to become the main component in the reaction mixture, amounting to 75 % of

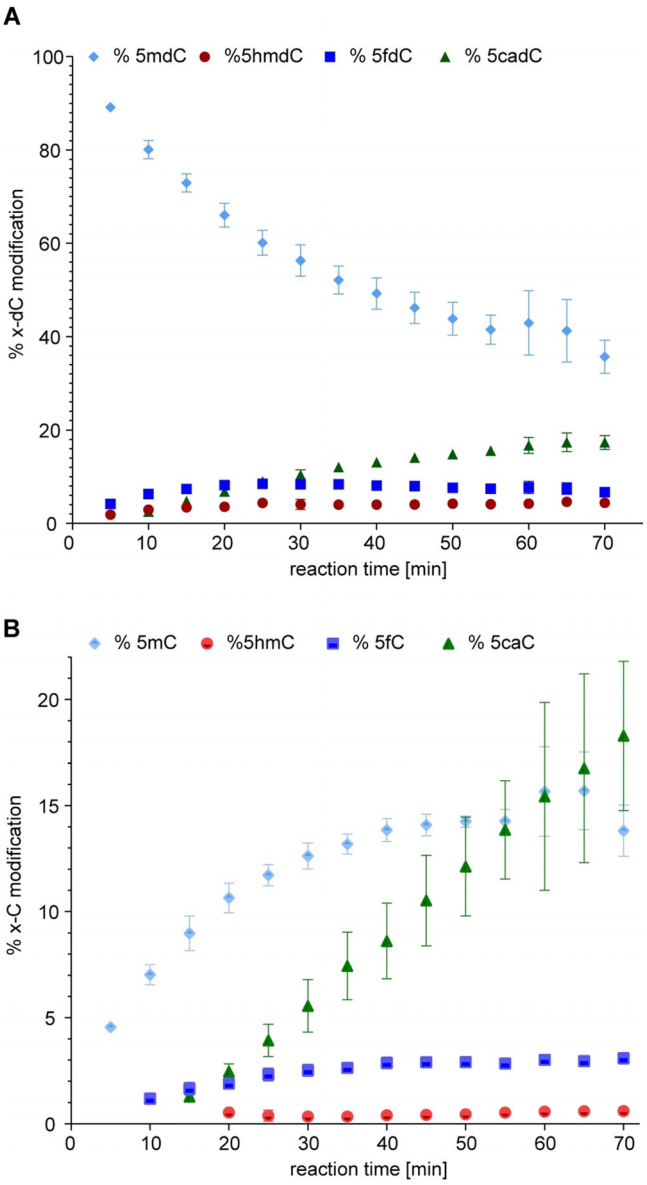

Figure 6. Time-resolved monitoring of the reaction products formed in the reaction of 5mdC with **1**: A) detected amounts of 5mdC, 5hmdC, 5fdC, 5cadC after certain time intervals; B) detected amounts of 5mC, 5hmC, 5fC and 5caC. Conditions: [5mdC] = 1.0 mM, [**1**] = 5.0 mM, H_2O, T = 22 °C. Data points are averaged from three replicates.

recovered products after 70 min. Remarkably, the amount of nucleosides recovered remained at high proportions of the products recovered in total throughout the entire course of the reaction, again indicating that $C_{1'}$ oxidation was significantly slower than the oxidation of the respective 5-substituents.

A further control reaction was performed with 5-[D_3]-mdC (D_3-5mdC, for synthesis procedure see section 4 SI) as substrate for **1** (Figures S25, S26, Scheme S3), which should be oxidized very slowly at the 5-substituent and more preferably at $C_{1'}$ due to an expected kinetic isotope effect like we had previously observed for the nucleobases.[27] Indeed, only very low levels (under limit of quantification) of both 5-oxidised nucleosides and nucleobases were found even after 70 min. This kinetic isotope effect added more evidence for the consensus radical mechanism involving hydrogen atom abstraction as the rate-limiting step. While the amount of starting material decreased very slowly, D_3-5mC accumulated to about 21 % in the reaction mixture after 65 min. At the same time, the reaction solution retained a green color rather than the orange appearance it adopted with 5mdC and 5hmdC as substrates, both suggesting low consumption of **1** when the reaction with the cytosine 5-substituent is markedly slowed down.

The experiments with **1** and different nucleosides as substrates demonstrate conclusively that the most reactive position on the nucleoside is the 5-substituent of the nucleobase, modulated by its oxidation state. The anomeric center, on the other hand, appears less prone to oxidation by **1**, despite its lower BDE compared to the methyl group in 5mC or the formyl group in 5fC. This indicates that the $C_{1'}$ hydrogen atom is hindered by steric interactions while the base modification is easily accessible. The results are in line with the observations discussed above for oligonucleotide substrates, where elimination reactions caused by oxidation of the sugar backbone—which is significantly more sterically demanding than a single nucleoside sugar—occurred only marginally and, if, only at the terminal nucleotides.

Conclusion

We have provided clear evidence that the fully-synthetic biomimetic iron(IV)-oxo complex **1** achieved TET enzyme reactivity: the epigenetic marker 5mdC is oxidized to the corresponding TET metabolites 5hmdC, 5fdC, and 5cadC within an oligonucleotide context (albeit at relatively large concentrations of 0.125–0.25 mM). We monitored the product distribution for different amounts of **1** and its development over time. In these reactions, we observed few side products showing the high specificity of **1** toward oxidation of the 5-position on the cytosine moiety. The side reaction we observed, loss of a cytosine or guanine nucleobase, occurs only at the ends of the 10-mer oligonucleotide substrate. We postulate that oxidation at the 1′ position of deoxyribose forms a lactone and releases the nucleobase. This is supported by our studies of the reactivity of **1** towards nucleoside substrates 5mdC and 5hmdC. Here, we observed oxidation of the 5-position on the cytosine moiety to the expected derivatives (5hmdC/5fdC/5cadC). In addition, we found that 1′ oxidation occurs very slowly, producing the corresponding nucleobases and 2′-deoxyribono-γ-lactone, confirming our hypothesis concerning the oligonucleotide side reactions. Further studies should include longer and more complex oligonucleotides and double stranded substrates. In addition, the influence of the amount of **1** and the reaction time on product composition needs to be investigated as a potential tool for epigenetic sequencing.

Acknowledgements

A grant from the Deutsche Forschungsgemeinschaft (DFG, German Research Foundation)—SFB 1309-325871075 is gratefully acknowledged. NSWJ thankfully acknowledges financial support by a scholarship of the Studienstiftung des Deutschen Volkes. NSWJ also thanks Juliane Kamlah and Doreen Reuters neé Kremer for their contributions and Prof. Stefanie Kellner for helpful discussions. Open access funding enabled and organized by Projekt DEAL.

Conflict of Interest

The authors declare no conflict of interest.

Keywords: 5-methyl cytosine · bioinorganic chemistry · DNA methylation · enzyme models · iron(IV)-oxo · TET enzymes

[1] M. V. C. Greenberg, D. Bourc'his, *Nat. Rev. Mol. Cell Biol.* **2019**, *20*, 590 – 607.
[2] Y. He, J. R. Ecker, *Annu. Rev. Genomics Hum. Genet.* **2015**, *16*, 55 – 77.
[3] A. M. Deaton, A. Bird, *Genes Dev.* **2011**, *25*, 1010 – 1022.
[4] T. Carell, M. Q. Kurz, M. Müller, M. Rossa, F. Spada, *Angew. Chem. Int. Ed.* **2018**, *57*, 4296 – 4312; *Angew. Chem.* **2018**, *130*, 4377 – 4394.
[5] E. Habibi, A. B. Brinkman, J. Arand, L. I. Kroeze, H. H. D. Kerstens, F. Matarese, K. Lepikhov, M. Gut, I. Brun-Heath, N. C. Hubner, R. Benedetti, L. Altucci, J. H. Jansen, J. Walter, I. G. Gut, H. Marks, H. G. Stunnenberg, *Cell Stem Cell* **2013**, *13*, 360 – 369.
[6] Z. D. Smith, A. Meissner, *Nat. Rev. Genet.* **2013**, *14*, 204 – 220.
[7] M. Tahiliani, K. P. Koh, Y. Shen, W. A. Pastor, H. Bandukwala, Y. Brudno, S. Agarwal, L. M. Iyer, D. R. Liu, L. Aravind, A. Rao, *Science* **2009**, *324*, 930 – 935.
[8] S. Ito, L. Shen, Q. Dai, S. C. Wu, L. B. Collins, J. A. Swenberg, C. He, Y. Zhang, *Science* **2011**, *333*, 1300 – 1303.
[9] Y.-F. He, B.-Z. Li, Z. Li, P. Liu, Y. Wang, Q. Tang, J. Ding, Y. Jia, Z. Chen, L. Li, Y. Sun, X. Li, Q. Dai, C.-X. Song, K. Zhang, C. He, G.-L. Xu, *Science* **2011**, *333*, 1303 – 1307.
[10] F. Spada, S. Schiffers, A. Kirchner, Y. Zhang, G. Arista, O. Kosmatchev, E. Korytiakova, R. Rahimoff, C. Ebert, T. Carell, *Nat. Chem. Biol.* **2020**, *16*, 1411 – 1419.
[11] A. Schön, E. Kaminska, F. Schelter, E. Ponkkonen, E. Korytiaková, S. Schiffers, T. Carell, *Angew. Chem. Int. Ed.* **2020**, *59*, 5591 – 5594; *Angew. Chem.* **2020**, *132*, 5639 – 5643.
[12] E. L. Hegg, L. Que, *Eur. J. Biochem.* **1997**, *250*, 625 – 629.
[13] L. Hu, Z. Li, J. Cheng, Q. Rao, W. Gong, M. Liu, Y. G. Shi, J. Zhu, P. Wang, Y. Xu, *Cell* **2013**, *155*, 1545 – 1555.

[14] J. C. Price, E. W. Barr, B. Tirupati, J. M. Bollinger, C. Krebs, *Biochemistry* **2003**, *42*, 7497 – 7508.
[15] P. J. Riggs-Gelasco, J. C. Price, R. B. Guyer, J. H. Brehm, E. W. Barr, J. M. Bollinger, C. Krebs, *J. Am. Chem. Soc.* **2004**, *126*, 8108 – 8109.
[16] M. L. Neidig, C. D. Brown, K. M. Light, D. G. Fujimori, E. M. Nolan, J. C. Price, E. W. Barr, J. M. Bollinger, C. Krebs, C. T. Walsh, E. I. Solomon, *J. Am. Chem. Soc.* **2007**, *129*, 14224 – 14231.
[17] S. Kal, L. Que, *J. Biol. Inorg. Chem.* **2017**, *22*, 339 – 365.
[18] P. A. MacFaul, K. U. Ingold, D. D. M. Wayner, L. Que, *J. Am. Chem. Soc.* **1997**, *119*, 10594 – 10598.
[19] M. Costas, K. Chen, L. Que, *Coord. Chem. Rev.* **2000**, *200 – 202*, 517 – 544.
[20] C. R. Goldsmith, R. T. Jonas, T. D. P. Stack, *J. Am. Chem. Soc.* **2002**, *124*, 83 – 96.
[21] M. R. Bukowski, K. D. Koehntop, A. Stubna, E. L. Bominaar, J. A. Halfen, E. Münck, W. Nam, L. Que, *Science* **2005**, *310*, 1000 – 1002.
[22] A. N. Biswas, M. Puri, K. K. Meier, W. N. Oloo, G. T. Rohde, E. L. Bominaar, E. Münck, L. Que, *J. Am. Chem. Soc.* **2015**, *137*, 2428 – 2431.
[23] J. E. M. N. Klein, L. Que, *Encyclopedia of Inorganic and Bioinorganic Chemistry*, American Cancer Society, Atlanta, **2016**, pp. 1 – 22.
[24] R. J. Martinie, C. J. Pollock, M. L. Matthews, J. M. Bollinger, C. Krebs, A. Silakov, *Inorg. Chem.* **2017**, *56*, 13382 – 13389.
[25] T. Chantarojsiri, Y. Sun, J. R. Long, C. J. Chang, *Inorg. Chem.* **2015**, *54*, 5879 – 5887.
[26] L. Hu, J. Lu, J. Cheng, Q. Rao, Z. Li, H. Hou, Z. Lou, L. Zhang, W. Li, W. Gong, M. Liu, C. Sun, X. Yin, J. Li, X. Tan, P. Wang, Y. Wang, D. Fang, Q. Cui, P. Yang, C. He, H. Jiang, C. Luo, Y. Xu, *Nature* **2015**, *527*, 118 – 122.
[27] N. S. W. Jonasson, L. Daumann, *Chem. Eur. J.* **2019**, *25*, 12091 – 12097.
[28] M. J. Booth, M. R. Branco, G. Ficz, D. Oxley, F. Krueger, W. Reik, S. Balasubramanian, *Science* **2012**, *336*, 934 – 937.
[29] W. Mao, J. Hu, T. Hong, X. Xing, S. Wang, X. Chen, X. Zhou, *Org. Biomol. Chem.* **2013**, *11*, 3568 – 3572.
[30] M. J. Booth, G. Marsico, M. Bachman, D. Beraldi, S. Balasubramanian, *Nat. Chem.* **2014**, *6*, 435 – 440.
[31] B. Xia, D. Han, X. Lu, Z. Sun, A. Zhou, Q. Yin, H. Zeng, M. Liu, X. Jiang, W. Xie, C. He, C. Yi, *Nat. Methods* **2015**, *12*, 1047 – 1050.
[32] C. Zhu, Y. Gao, H. Guo, B. Xia, J. Song, X. Wu, H. Zeng, K. Kee, F. Tang, C. Yi, *Cell Stem Cell* **2017**, *20*, 720 – 731.e5.
[33] M. Frommer, L. E. McDonald, D. S. Millar, C. M. Collis, F. Watt, G. W. Grigg, P. L. Molloy, C. L. Paul, *Proc. Natl. Acad. Sci. USA* **1992**, *89*, 1827 – 1831.
[34] A. M. Raizis, F. Schmitt, J. P. Jost, *Anal. Biochem.* **1995**, *226*, 161 – 166.
[35] K. Tanaka, A. Okamoto, *Bioorg. Med. Chem. Lett.* **2007**, *17*, 1912 – 1915.
[36] Y. Huang, W. A. Pastor, Y. Shen, M. Tahiliani, D. R. Liu, A. Rao, *PLoS One* **2010**, *5*, e8888.
[37] C. Nestor, A. Ruzov, R. Meehan, D. Dunican, *Biotechniques* **2010**, *48*, 317 – 319.
[38] S.-G. Jin, S. Kadam, G. P. Pfeifer, *Nucleic Acids Res.* **2010**, *38*, e125.
[39] M. Yu, G. C. Hon, K. E. Szulwach, C.-X. Song, L. Zhang, A. Kim, X. Li, Q. Dai, Y. Shen, B. Park, J.-H. Min, P. Jin, B. Ren, C. He, *Cell* **2012**, *149*, 1368 – 1380.
[40] M. Yu, G. C. Hon, K. E. Szulwach, C.-X. Song, P. Jin, B. Ren, C. He, *Nat. Protoc.* **2012**, *7*, 2159 – 2170.
[41] Y. Liu, P. Siejka-Zielińska, G. Velikova, Y. Bi, F. Yuan, M. Tomkova, C. Bai, L. Chen, B. Schuster-Böckler, C.-X. Song, *Nat. Biotechnol.* **2019**, *37*, 424 – 429.
[42] K. C. Cheng, D. S. Cahill, H. Kasai, S. Nishimura, L. A. Loeb, *J. Biol. Chem.* **1992**, *267*, 166 – 172.
[43] S. Kanvah, J. Joseph, G. B. Schuster, R. N. Barnett, C. L. Cleveland, U. Landman, *Acc. Chem. Res.* **2010**, *43*, 280 – 287.
[44] F. Boussicault, M. Robert, *Chem. Rev.* **2008**, *108*, 2622 – 2645.
[45] S. Steenken, S. V. Jovanovic, L. P. Candeias, J. Reynisson, *Chem. Eur. J.* **2001**, *7*, 2829 – 2833.
[46] M. Sako, T. Kihara, H. Kawada, K. Hirota, *J. Org. Chem.* **1999**, *64*, 9722 – 9723.
[47] V. A. Stepchenko, F. Seela, R. S. Esipov, A. I. Miroshnikov, Y. A. Sokolov, I. A. Mikhailopulo, *Synlett* **2012**, *23*, 1541 – 1545.

Manuscript received: May 31, 2021
Revised manuscript received: June 23, 2021
Accepted manuscript online: June 28, 2021
Version of record online: August 20, 2021

